Appl. Phys. B 74, 607–611 (2002)
DOI: 10.1007/s003400200845

Applied Physics B
Lasers and Optics

I.T. SOROKINA[1,✉]
E. SOROKIN[1]
S. MIROV[2]
V. FEDOROV[2]
V. BADIKOV[3]
V. PANYUTIN[3]
A. DI LIETO[4]
M. TONELLI[4]

Continuous-wave tunable Cr^{2+}:ZnS laser

[1] Institut für Photonik, TU Wien, Gusshausstr. 27/ 387, 1040 Vienna, Austria
[2] Deptartment of Physics, University of Alabama at Birmingham, 1300 University Blvd., Birmingham, AL 35244-1170, USA
[3] Kuban State University, 149 Stavropolskaya str., Krasnodar, 350040, Russia
[4] INFM, Dipartimento di Fisica, University of Pisa,Via Buonarotti 2, 56127 Pisa, Italy

Received: 7 January 2002/Revised: 14 March 2002
Published online: 2 May 2002 •

ABSTRACT We report the first continuous-wave tunable over ∼ 280 nm around 2.3 μm room-temperature operation of a chemical vapor transport-grown and diffusion-doped Cr^{2+}:ZnS laser, pumped by a Co:MgF_2 laser at 1.67 μm and generating over 100 mW of output power at 16% slope efficiency. The self-consistent results of the laser and spectroscopic analysis demonstrate a large potential of this crystal as an active medium for diode-pumped tunable mid-infrared sources.

PACS 42.70.Hj; 42.55.Rz

A new class of the transition-metal-doped chalcogenides [1–4], and in particular Cr:ZnSe, has recently become the subject of active research because of the successful use of these materials as active media of the broadly tunable continuous-wave (cw) lasers operating around 2.5 μm [5–7]. This interest is explained by the excellent laser properties as well as by the promising outlook for the use of these materials in a variety of applications, such as environmental analysis, remote sensing, spectroscopy, and medicine. Among this class of lasers, continuous-wave room-temperature Cr:ZnSe has demonstrated the highest reported so far for transition-metal-doped lasers slope efficiency (> 60% [5, 7, 12]) and output power (> 1.8 W [8]), coverage of the whole 2 − 3.1-μm wavelength range [9], as well as diode pumping [10–12]. At the same time, another member of the II–VI-compound family Cr:ZnS [1, 2], which is in many respects similar to Cr:ZnSe, has yet remained barely studied as a laser material, maybe due to the lack of good optical quality single crystals. Having spectroscopic properties similar to Cr:ZnSe, the Cr:ZnS crystal is known to have the larger band gap (compare 3.84 eV in ZnS and 2.83 eV in ZnSe [13]), the better hardness, the higher thermal conductivity in the cubic phase (27 W/mK in ZnS vs. 19 W/mK in ZnSe [14]), the higher thermal shock parameter (7.1 $W/m^{1/2}$ in ZnS vs. 5.3 $W/m^{1/2}$ in ZnSe [1]), and the lower dn/dT ($+46 \times 10^{-6}\,K^{-1}$ in ZnS vs. $+70 \times 10^{-6}\,K^{-1}$ in ZnSe [1]). Therefore, the power-handling capability of this material should be higher than that of Cr:ZnSe, making Cr:ZnS attractive for high-power applications. The profound spectroscopic investigation and the pulsed laser operation of the Cr:ZnS laser has been first reported in [1, 2, 15].

In this communication we report the first tunable in the water-free window around 2.3 μm continuous-wave operation of a Cr:ZnS laser pumped by a Co:MgF_2 laser at 1.67 μm.

The ZnS crystal has been grown by the chemical vapor transport (CVT) method and afterwards diffusion-doped with chromium as described in [15]. The sample was a 1-mm-thick slightly wedged (0.4 degrees) rectangular $5 \times 5\,mm^2$ plate, which was antireflection (AR)-coated (between ∼ 2.2 and 2.8 μm) on both sides. After correction for the considerable reflection present at the pumping wavelength the crystal was found to absorb about 43% of the incident pump light at 1.67 μm.

X-ray analysis revealed the hexagonal symmetry in our crystal, although the structure turned out to be not that of wurtzite, but a modification of the cubic structure. It is worth noting that ZnS is one of the most structurally rich chalcogenide compounds. Besides the two basic wurtzite (hexagonal) and zinc blende (cubic) structures [16], a number of the so-called mixed-polytype structures [17] are common for ZnS. In the latter case the stacking order of successive anion and cation planes along the hexagonal [001] c axis (which corresponds to the cubic [111] axis) is disturbed and the repeating periods are longer. There are many factors influencing the mixed-polytype formation and the degree of hexagonality in such crystals (for details see e.g. [18]). Those include: temperature of crystallization, which is generally higher in ZnS than in ZnSe, thermal treatment, stress, pressure, as well as doping, in particular with Cr ions [19, 20]. The difficulty to develop a purely cubic Cr:ZnS seems to be a basic problem of this material, which may need special efforts of crystal growers in order to be solved. At the moment, the exact structural type of our crystal and its degree of "hexagonality" are unknown, as this requires an elaborated structural analysis. From the point of view of laser physics the issue of hexagonality has three main consequences: (i) the intrinsic birefringence of the crystal, (ii) anisotropy in Cr^{2+} absorption and emission spectra,

✉ Fax: +43-1/58801-38799, E-mail: sorokina@tuwien.ac.at

and (iii) somewhat lower thermal conductivity than in a purely cubic crystal (compare 27 W/mK in cubic ZnS and 17 W/mK in hexagonal ZnS [14]). Both birefringence and polarization dependence of luminescence can be considered as advantageous features of the laser medium [21], while lower thermal conductivity presents an obvious problem for high-power applications.

The room-temperature absorption and fluorescence spectra of the studied Cr:ZnS crystal are given in cross-sectional units in Fig. 1. The absorption spectrum was measured using the "Cary 5" spectrophotometer. The fluorescence spectrum was measured using the Acton Research ARC-300i spectrometer and a PbS detector. The spectrum was corrected with respect to the spectral sensitivity of the recording system using the tungsten–halogen lamp (Oriel 9-2050). As an excitation source we used a cw erbium-doped fiber laser (IPG Group ELD-2), modulated at 800 Hz. The measured gain spectrum is similar to the spectrum reported in the first publication on the Cr:ZnS laser [1]. The slight difference in the spectral shape can be attributed to the above-mentioned difference in the crystal structure between crystals grown by different methods, i.e. the CVT method in this work and Bridgman growth in [1]. The presence of the "hexagonal" lines (doublet of the zero-phonon lines [22]) in the low-temperature absorption and emission spectra has been earlier revealed in the crystal, which was grown similarly to our sample [15]. Since the polarization degree depends upon crystal structure and growth conditions, anisotropic effects should be always kept in mind and carefully considered in each particular case. However, we should note that the difference due to the polarization dependence of the absorption and fluorescence spectra in our case did not exceed 10% at room temperature. This allowed us (similarly to other authors) to treat the studied crystal in the first approximation as optically isotropic.

The luminescence kinetics measured at $\lambda = 1950$ nm across a broad temperature range using Raman-shifted Nd:YAG laser excitation at 1560 nm are given in Fig. 2. The InSb detector with a time resolution of 0.5 μs was used in the experiments. The emission lifetime drops only slightly, i.e. from 5.7 to 4.3 μs, between 14 and 300 K (Fig. 3). This shows that quenching is not important below 300 K. This observation is consistent with the earlier reports [23]. However, we should note that the lifetime values are lower than previously reported in [1]. The further heating of the crystal leads to the drastic decrease of the lifetime, and at 450 K it was already limited by the detector time constant. Using the lifetime temperature dependence (Fig. 3) we could estimate the activation energy for the non-radiative decay from the excited state

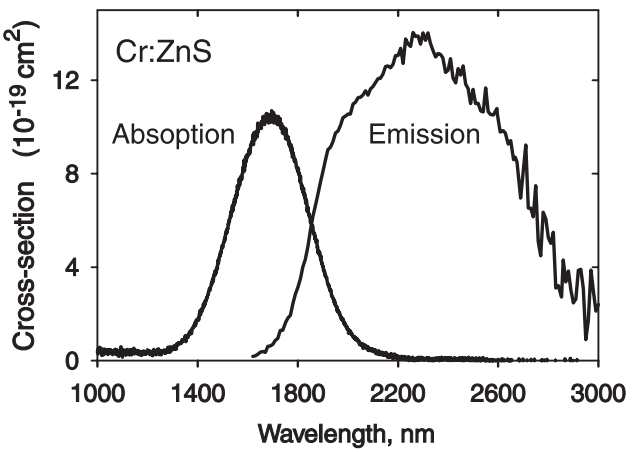

FIGURE 1 Cr:ZnS absorption and emission spectra measured at 300 K and plotted in cross-sectional units

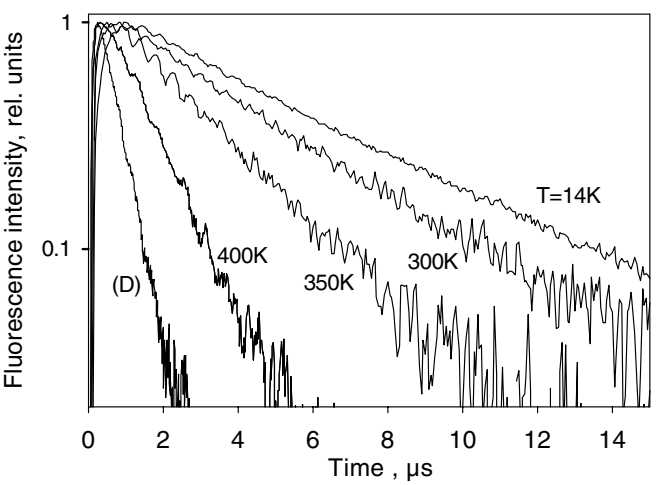

FIGURE 2 Kinetics of ZnS fluorescence measured at different temperatures. The *curves* labels correspond to the temperatures in K. The *curve* (D) shows the detector's time response

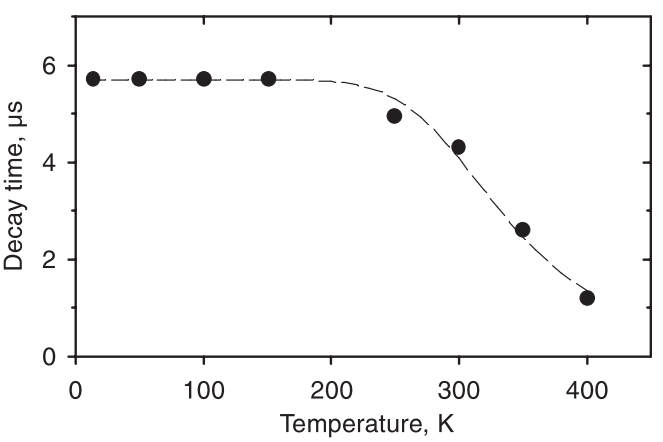

FIGURE 3 Emission lifetime temperature dependence measured at $\lambda = 1950$ nm

to the ground state to be of the order of $\sim 2000\,\mathrm{cm}^{-1}$. This value is well above both the kT energy at room temperature and the highest phonon energy in ZnS.

The spontaneous emission cross section $\sigma_{\mathrm{em}}(\lambda)$ (Fig. 1) was obtained from the fluorescence intensity signal $I(\lambda)$ (measured in energy units with a constant slit width in wavelength space) using the relation

$$\sigma_{\mathrm{em}}(\lambda) = \frac{A}{8\pi c n^2} \frac{I(\lambda)\lambda^5}{\int I(\lambda)\lambda \mathrm{d}\lambda}, \qquad (1)$$

where A is the full spontaneous emission probability from the upper laser level and n is the index of refraction of ZnS ($n = 2.27$ around 2.3 μm). Formula (1) follows from the basic principles [24, 25] and does not contain assumptions other than neglecting the polarization dependence of fluorescence, which is accurate within $\sim 10\%$ as mentioned above. Taking the inverse lifetime at low temperature as a best-known approximation for the radiative decay rate, we obtain $\sigma_{\mathrm{em}} = 1.4 \times 10^{-18}\,\mathrm{cm}^2$ at $\lambda = 2330\,\mathrm{nm}$. To derive the absorption cross-sectional magnitude from the absorption spectrum, one needs to know the Cr^{2+} concentration. Unfortunately, the absolute dopant concentration is neither uniform nor accurately known in the case of diffusion doping. We therefore used the reciprocity relation for the four-level broad-band transition $\int \sigma_{\mathrm{em}}(\nu)\mathrm{d}\nu = (g_1/g_2) \int \sigma_{\mathrm{abs}}(\nu)\mathrm{d}\nu$ [25] to calculate the absorption cross section in Fig. 1, making use of the known ground- and upper-level degeneracies $g_1 = 3$ and $g_2 = 2$, respectively. In contrast to Ti:sapphire [25], we neglect the Jahn–Teller splitting of both levels, as it is less than or comparable to kT at room temperature ($\sim 300\,\mathrm{cm}^{-1}$ for the $^5T_2$ ground state and $\sim 60\,\mathrm{cm}^{-1}$ for the $^5E_2$ upper state [26]). The magnitudes of the cross sections obtained this way are higher by a factor of ~ 2 than those previously reported [1]. This is a direct consequence of the ~ 2 times shorter radiative lifetime which we measured and used in the calculation (1) (5.7 μs vs. 11 μs in [1]). At the same time, our value for the peak absorption cross section of $\sigma_{\mathrm{abs}} = 1.0 \times 10^{-18}\,\mathrm{cm}^2$ at $\lambda = 1690\,\mathrm{nm}$ agrees well with the value of $\sigma_{\mathrm{abs}} = 1.2 \times 10^{-18}\,\mathrm{cm}^2$ obtained using the absorption coefficient and the known concentration of Cr^{2+} in [27].

The laser cavity (Fig. 4) was formed by the crystal, which was fixed on a room-temperature copper block, the flat dichroic mirror with $R = 50\,\mathrm{mm}$ radius of curvature, and the plane output coupler, varying between 1 and 20%, the optimum being $\sim 10\%$. The sample was oriented to oscillate along the [001] axis, i.e. the crystal c axis (which coincides with a cubic [111] direction for zinc blende). The AR coatings and other intracavity optics were centered at ~ 2.35 μm. Our pump source was a continuous-wave liquid nitrogen cooled polarized Co:MgF_2 laser [28], tunable between 1.62 and 2.13 μm [7]. The broad tuning range allowed us to pump Cr:ZnS at the maximum of the Cr^{2+} absorption band at 1.67 μm. The pump power coupled into the Cr:ZnS cavity was adjusted by the variable attenuator, consisting of the two Brewster-angled ZnSe plates, rotating around the beam axis. The pump radiation was polarized parallel to the c axis of the crystal. The Co:MgF_2 laser was focused onto the crystal by the uncoated lens of 75-mm focal length into the spot size smaller than 60 μm in diameter. The resonator beam spot size was calculated to be ~ 60 μm in the middle of the stability range.

The laser output characteristics are given in Fig. 5. The laser could be brought to lasing with the output-coupler transmission as high as 20%, but a maximum output power of $\sim 100\,\mathrm{mW}$ at $\sim 0.9\,\mathrm{W}$ of absorbed power was reached with a 10% output coupler. The output was polarized along the c axis, and the laser mode was close to TEM00. The slope efficiency was measured to be $\sim 16\%$ and was probably set by the non-optimal beam overlap within the crystal. We should note that, in this pump configuration, the Cr:ZnS crystal easily falls into a coupled-cavity Q-switching regime with the Co:MgF_2 laser, as was reported for Cr:ZnSe [7]. The parasitic reflection was coming from the rear surface of the crystal, and without the optical isolator could only be avoided by oblique incidence or lateral shift of the pump focal plane away from the crystal. In practice we had to readjust the pump beam during the experiment to avoid the Q-switching, sacrificing the optimal overlap. To get rid of this prob-

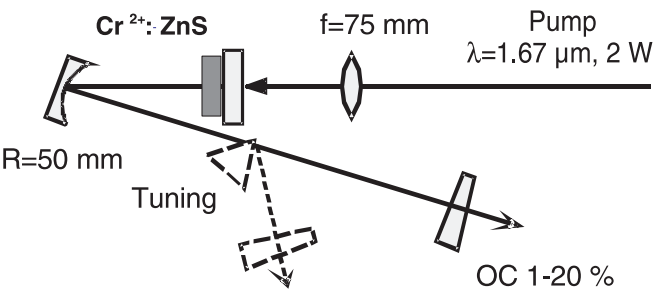

FIGURE 4 Schematic of the experimental setup. The pump at 1.67 μm and the output radiation at 2.35 μm are polarized in the plane of the figure. OC, output coupler; F, focusing lens

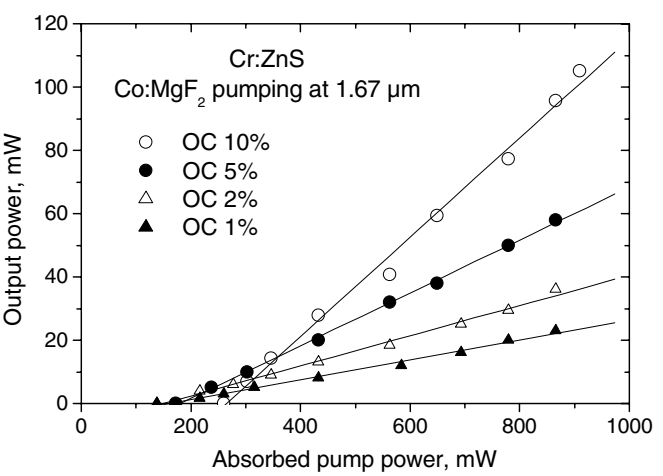

FIGURE 5 Output characteristics of the Cr:ZnS laser

lem, one needs to use the optical isolator or the backreflection-free geometry, e.g. a Brewster-oriented crystal. We should also note that while lasing in the free-running regime (without any selective elements inside the cavity) at $\sim 2.35\,\mu$m the laser operated at the maximum of its gain. We do not observe any deterioration of the output power due to the thermal loading up to the absorbed pump power level of ~ 0.9 W, a result of the good thermal conductivity of Cr:ZnS. Using the inverse slope efficiency analysis [29] we measured the passive losses of the crystal to be 5% per round trip, i.e. 25%/cm. These losses also include the losses on the coatings and agree with the spectrophotometer measurements. Nevertheless they are still noticeably higher than the corresponding values for Cr:ZnSe ($\sim 4\%$/cm [7]). The threshold was measured to be 140 mW of absorbed power at 1% output coupling. However, at the similar cavity parameters Cr:ZnSe exhibits only a few tens of mW threshold. Taking the room-temperature lifetime measured in our crystal to be $\sim 4.3\,\mu$s and the emission cross section to be $\sim 14 \times 10^{-19}\,\mathrm{cm}^2$, we obtain a saturation intensity value for Cr:ZnS $I_s \sim 14\,\mathrm{kW/cm}^2$, which is the same as the corresponding value in Cr:ZnSe ($14\,\mathrm{kW/cm}^2$ [2]). The calculated threshold (assuming optimal pump beam overlap) in both lasers is as low as ~ 20 mW. We thus believe that the higher threshold in Cr:ZnS is due to the higher passive losses of the studied crystal and non-optimal overlap. With the progress in crystal growth of Cr:ZnS and provided that the low-loss crystals become available, diode pumping of this material should not be a problem.

Using a dry fused-silica Brewster prism as a tuning element, we were able to demonstrate tunability over ~ 280 nm: from 2188 to 2465 nm (Fig. 6). This falls into the range of the measured emission cross-section spectrum (Fig. 1). The tuning range was obviously limited by the AR coatings on the crystal and can certainly be extended in the future, especially towards the blue side. On the long-wavelength side, the water vapor inside the resonator hinders tuning beyond 2650 nm [7].

Summarizing, we demonstrated the first continuous-wave tunable Cr:ZnS laser, using the CVT-grown single crystal. It is interesting to note that the first reports on pulsed lasing in Cr:ZnS [1, 2, 15] did not reveal any polarization dependence, and this is the first report to our knowledge on this kind of behavior in Cr:ZnS. A more detailed investigation of the observed polarization dependence will be given in a following publication. The observed reasonably low threshold of 140 mW of absorbed power and availability of the high-brightness pump laser diodes at 1.6 μm render the diode pumping of this material possible. Assuming that the excited-state absorption should be negligible in this crystal [1, 12], the improved crystal quality and optimal pump design should increase slope efficiency in excess of 50%. There still remain crystal-growth challenges to overcome before the large-size crystals of the same quality as Cr:ZnSe can be routinely grown. However, the reported results demonstrate a high potential of Cr:ZnS for compact high-power continuous-wave tunable mid-infrared laser sources.

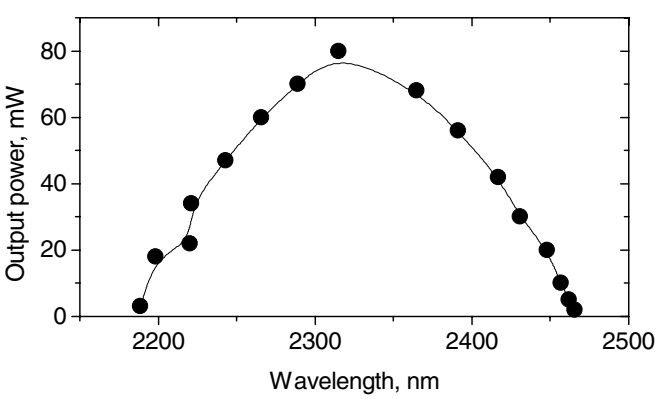

FIGURE 6 Tuning range of the Cr:ZnS laser

ACKNOWLEDGEMENTS This work has been performed under the Austrian Fonds zur Förderung der Wissenschaftlichen Forschung (Grant Nos. T64 and P14704-TPH) and BMBWK Grant No. B631. We would also like to thank Prof. Kurt Mereiter, Department of Chemistry, TU Wien, for the X-ray analysis.

Note added in proof. Recently we demonstrated direct diode-pumping at 1.6 μm of Cr:ZnS, yielding 25 mW of cw output power at room temperature, tunable betweeen 2250 and 2650 nm.

REFERENCES

1 L.D. DeLoach, R.H. Page, G.D. Wilke, S.A. Payne, W.F. Krupke: IEEE J. Quantum Electron. **QE-32**, 885 (1996)
2 R.H. Page, K.I. Schaffers, L.D. DeLoach, G.D. Wilke, W.F. Krupke, J.B. Tassano, S.A. Payne, F.D. Patel, K.-T. Chen, A. Burger: IEEE J. Quantum Electron. **QE-33**, 609 (1997)
3 U. Hömmerich, X. Wu, V.R. Davis, S.B. Trivedi, K. Grasze, R.J. Chen, S.W. Kutcher: Opt. Lett. **22**, 1186 (1997)
4 J. McKay, K.L. Schepler, G.C. Catella: Opt. Lett. **24**, 1575 (1999)
5 G.J. Wagner, T.J. Carrig, R.H. Page, K.I. Schaffers, J. Ndap, X. Ma, A. Burger: Opt. Lett. **24**, 19 (1999)
6 A. Sennaroglu, A.O. Konca, C.R. Pollock: IEEE J. Quantum Electron. **QE-36**, 1199 (2000)
7 I.T. Sorokina, E. Sorokin, A. DiLieto, M. Tonelli, R.H. Page, K.I. Schaffers: JOSA B **18**, 926 (2001)
8 G.J. Wagner, T.J. Carrig: *OSA Trends in Optics and Photonics on Advanced Solid-State Lasers, Vol. 46*, ed. by S. Payne, C. Marshall (Optical Society of America, Washington, DC 2001) pp. 506–510
9 I.T. Sorokina, E. Sorokin, A. DiLieto, M. Tonelli, R.H. Page: Dig. *Conf. Lasers Electro-Opt./Europe 2001, Munich, 2001*, p. 151 (oral presentation)
10 R.H. Page, J.A. Skidmore, K.I. Schaffers, R.J. Beach, S.A. Payne, W.F. Krupke: *OSA Trends in Optics and Photonics*, ed. by C.R. Pollock, W.R. Bosenberg (OSA, Washington, DC 1997) pp. 208–210
11 E. Sorokin, I.T. Sorokina, R.H. Page: *OSA Trends in Optics and Photonics on Advanced Solid-State Lasers, Vol. 46*, ed. by S. Payne, C. Marshall (Optical Society of America, Washington, DC 2001) pp. 101–105
12 A.V. Podlipensky, V.G. Shcherbitsky, N.V. Kuleshov, V.I. Levchenko, V.N. Yakimovich, M. Mond, E. Heumann G. Huber, H. Kretschmann, S. Kück: Appl. Phys. B **72**, 253 (2001)
13 B. Segall, D.T.F. Marple: in *Physics and Chemistry of II–IV Compounds*, ed. by M. Aven, J.S. Prener (North Holland, Amsterdam 1967) pp. 319–381
14 G.A. Slack: Phys. Rev. B **6**, 3791 (1972)
15 K. Graham, S. Mirov, V. Fedorov, M.E. Zvanut, A. Avanesov, V. Badikov, B. Ignat'ev, V. Panutin, G. Shevirdyaeva: *OSA Trends in Optics and Photonics on Advanced Solid-State Lasers, Vol. 46*, ed. by S. Payne, C. Marshall (Optical Society of America, Washington, DC 2001) pp. 561–567

16 B. Ray: in *II–VI Compounds* (Pergamon, London, UK 1969) p. 3
17 T. Buch, B. Clerjaud, B. Lambert, P. Kovacs: Phys. Rev. B **7**, 184 (1973)
18 A.R. Verma, P. Krishna: *Polymorphism and Polytypism in Crystals* (Wiley, New York 1966)
19 G.E. Arkhangel'skii, E.E. Bukke, M.V. Fok, N.N. Grigor'ev: J. Appl. Spectrosc. **50**, 406 (1989)
20 J. Gosk, M.J. Kozielski: Cryst. Res. Technol. **25**, 415 (1990)
21 B. Henderson, R.H. Bartram: *Crystal-field Engineering of Solid-state Laser Materials* (Cambridge University Press, Cambridge, UK 2000) p. 294
22 G. Grebe, H.-J. Schulz: Z. Naturforsch. **29a**, 1803 (1974)
23 R. Renz, H.-J. Schulz: J. Luminesc. **24–25**, 221 (1981)
24 D.E. McCumber: Phys. Rev. A **134**, A299 (1964)
25 P.F. Moulton: JOSA B **3**, 125 (1986)
26 M. Kaminska, J.M. Baranovski, S.M. Uba, J.T. Vallin: J. Phys. C: Solid State Phys. **12**, 2197 (1979)
27 C.S. Kelley, F. Williams: Phys. Rev. B **QE-2**, 3 (1970)
28 P.F. Moulton: IEEE J. Quantum Electron. **QE-21**, 1582 (1985)
29 J.A. Caird, S.A. Payne, P.R. Staver, A.J. Ramponi, L.L. Chase, W.F. Krupke: IEEE J. Quantum Electron. **QE-24**, 1077 (1988)